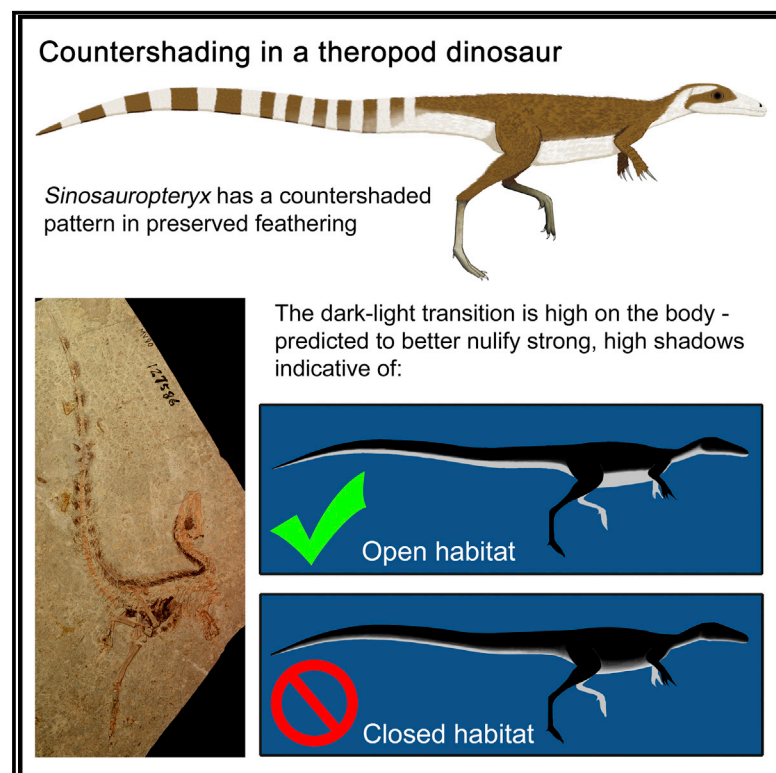


Current Biology

Countershading and Stripes in the Theropod Dinosaur *Sinosauropteryx* Reveal Heterogeneous Habitats in the Early Cretaceous Jehol Biota

Graphical Abstract



Authors

Fiann M. Smithwick, Robert Nicholls, Innes C. Cuthill, Jakob Vinther

Correspondence

jakob.vinther@bristol.ac.uk

In Brief

Smithwick et al. reconstruct the coloration of the small carnivorous dinosaur *Sinosauropteryx*. It had a bandit mask and striped tail and was also countershaded (dark on top, light below). Using 3D models under different light, the authors show that its camouflage would have worked best in an open habitat. Paleocolor can help predict paleohabitat.

Highlights

- We have reconstructed the color pattern of the theropod dinosaur *Sinosauropteryx*
- *Sinosauropteryx* exhibited camouflage, including countershading and a bandit mask
- The countershading pattern was most likely associated with an open habitat
- Previously assumed to be forested, Jehol likely included a range of habitat types



Countershading and Stripes in the Theropod Dinosaur *Sinosauropteryx* Reveal Heterogeneous Habitats in the Early Cretaceous Jehol Biota

Fiann M. Smithwick,¹ Robert Nicholls,² Innes C. Cuthill,³ and Jakob Vinther^{1,3,4,*}

¹School of Earth Sciences, University of Bristol, Wills Memorial Building, Queens Road, Bristol BS8 1RJ, UK

²Palaeocreations, 35 Hopps Road, Kingswood, Bristol BS15 9QQ, UK

³School of Biological Sciences, University of Bristol, Life Sciences Building, 24 Tyndall Avenue, Bristol BS8 1TQ, UK

⁴Lead Contact

*Correspondence: jakob.vinther@bristol.ac.uk

<https://doi.org/10.1016/j.cub.2017.09.032>

SUMMARY

Countershading is common across a variety of lineages and ecological time [1–4]. A dark dorsum and lighter ventrum helps to mask the three-dimensional shape of the body by reducing self-shadowing and decreasing conspicuousness, thus helping to avoid detection by predators and prey [1, 2, 4, 5]. The optimal countershading pattern is dictated by the lighting environment, which is in turn dependent upon habitat [1, 3, 5, 6]. With the discovery of fossil melanin [7, 8], it is possible to infer original color patterns from fossils, including countershading [3, 9, 10]. Applying these principles, we describe the pattern of countershading in the diminutive theropod dinosaur *Sinosauropteryx* from the Early Cretaceous Jehol Biota of Liaoning, China. From reconstructions based on exceptional fossils, the color pattern is compared to predicted optimal countershading transitions based on 3D reconstructions of the animal's abdomen, imaged in different lighting environments. Reconstructed patterns match well with those predicted for animals living in open habitats. Jehol is presumed to have been a predominantly closed forested environment [3, 11, 12], but our results indicate a more heterogeneous range of habitats. *Sinosauropteryx* is also shown to exhibit a “bandit mask,” a common pattern in many living vertebrates, particularly birds, that serves multiple functions including camouflage [13–18]. *Sinosauropteryx* therefore shows multiple color pattern features likely related to the habitat in which it lived. Our results show how reconstructing the color of extinct animals can inform on their ecologies beyond what may be obvious from skeletal remains alone.

RESULTS

Plumage Distribution

To reconstruct the color patterns of *Sinosauropteryx*, we analyzed three of the best-preserved specimens available

(Figures 1A and 1D and S1A). To reconstruct the color patterns accurately, first the distribution of pigmented plumage was described in detail for each specimen (Supplemental Descriptions). Each specimen shows extensive preservation of dark, presumably organically preserved fibers identified as feathers/feather homologs in distinct areas of the animal (Figures 1A and 1D and S1). Alternative interpretations of these structures as degraded skin collagen have recently been shown to be unfounded [19]. Preservation of feathers as organic films is due to the presence of the pigment melanin, and thus only originally pigmented feathers are found preserved in this manner [7, 8]. Visible absence of feathers in certain regions of the fossil is therefore likely due to unpigmented plumage that did not preserve, rather than a true absence of feathers in life [7, 8]. Alternatively, the areas lacking feathers could have been naked (there is no evidence of scales being preserved [19]) but would similarly be inferred to have been unpigmented. Because the feathering likely also served an insulatory role, an extensive distribution seems most plausible. Mapping the distribution of preserved pigmented feathers is therefore considered to reflect the extent of colored plumage on the animal, with other areas being covered by white (unpigmented) feathers.

Color Pattern Reconstruction

Illustrations of NIGP 127586 and NIGP 127587 show the pattern of plumage distribution across the fossils (Figures 1B and 1E). From this distribution, a complete reconstruction was created (Figure 2); this was done blind to any predictions from the modeling of illumination. The consistency of plumage patterns observed across multiple specimens gives confidence to the reconstructed color pattern. The pattern of pigment across the face appears to show a band of pigmented plumage running from the dorsal area of the head anteroventrally, which then angles toward the eye before running to the posteroventral margin of the lower jaw (Figures 3A–3E). The banded tail shows a transition from narrow to widely spaced bands from the proximal to distal regions, with the ventral pigmentation becoming denser toward the end of the tail. The ventral extent of the pigmented plumage, representing the likely countershading transition, appears to be relatively high on the flank, at around two-thirds of the way down the abdomen (Figures 3F–3I).



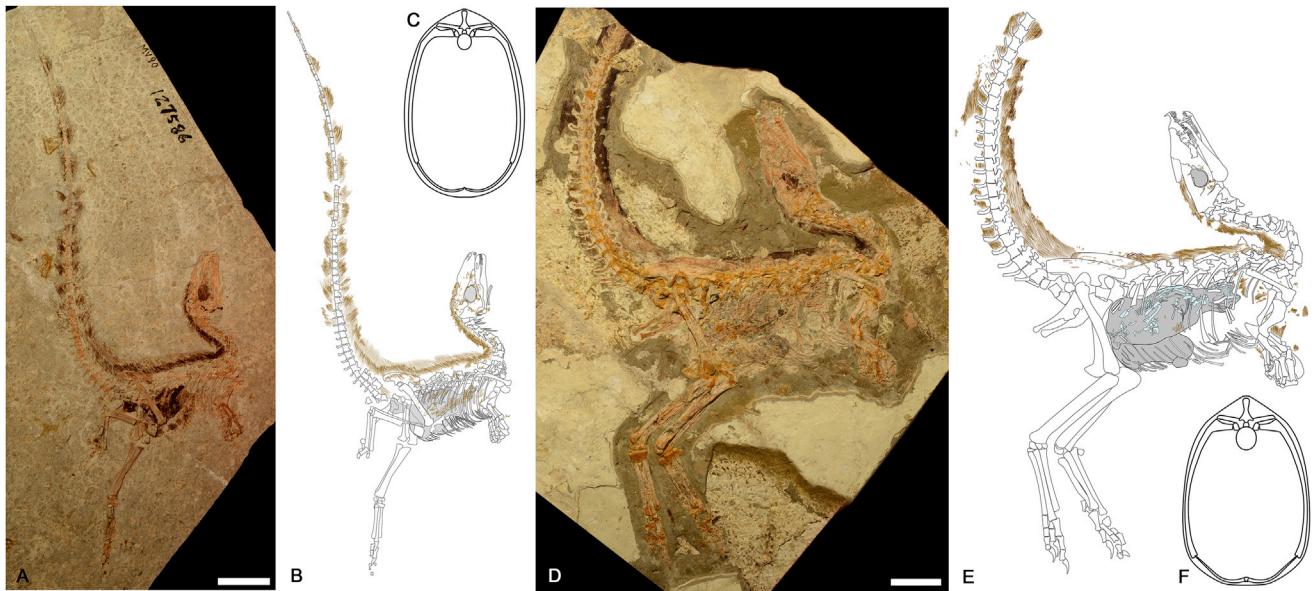


Figure 1. *Sinosauropteryx prima* Fossils and Interpretive Drawings

The plumage distribution is mapped out across each specimen, with feathers shown in brown, internal soft tissues and pigment from the eyes shaded gray, and vertebrate stomach contents in light blue. See also [Figures S1](#) and [S2](#).

(A) NIGP 127586 counterpart to the holotype.

(B) Interpretive drawing of NIGP 127586.

(C) Reconstructed transverse section through the abdomen of NIGP 127586.

(D) NIGP 127587.

(E) Interpretive drawing of NIGP 127587.

(F) Reconstructed cross-section through the abdomen of NIGP 127587. Scale bars represent 50 mm. Abdominal transverse sections not to scale.

Predicted Lighting Environment

For countershading to be effective in obliterating 3D cues of an animal's presence, the pattern of pigmentation from the dorsal to ventral body regions should match the illumination gradient created by the lighting environment in which it lives [1, 3, 5, 6]. This allows the determination of likely habitats of animals based on quantification of color patterns [1, 3]. Those that inhabit open environments with direct lighting conditions generally exhibit a sharp transition from dark to light color high up on the flanks of the body [1, 3]. Conversely, animals inhabiting a more closed habitat with diffuse lighting coming in at many angles often show a smoother gradation from dark to light lower down on the body [1, 3]. To predict the optimal pattern of countershading, we created and photographed 3D models of the abdomen of *Sinosauropteryx* under different lighting conditions. The reconstructed color patterns based on NIGP 127586 and NIGP 127587 ([Figures 2](#) and [3H–3I](#)) more closely match the pattern of countershading predicted from images of the models taken under direct light conditions than those of diffuse lighting conditions ([Figure 4](#)), indicative of animals living in open habitats [1, 3]. The addition of synthetic fur (representing feathers) made little difference to each countershading prediction ([Figure 4](#)). For direct overhead sun, the mean predicted transition point to lighter coloration was 72% (95% confidence interval [CI] 61%–83%) of the way from dorsal to ventral side. For direct sun at 30° it was 60% (95% CI 45%–75%), and for diffuse illumination it was 85% (95% CI 81%–88%). Only the direct illumination

confidence intervals include the observed transition point (~67%).

DISCUSSION

Color Patterns of the Face

The presence of pigmented feathers surrounding the orbit and running in a band across the face conforms to “bandit masks” seen in many modern birds and mammals [15–18]. Multiple functions have been proposed for bandit masks in modern taxa [13, 14, 16–18]. One such function is as an anti-glare device [15, 18]. Reducing the glare from the feathers around the eye would be particularly useful to an animal living in environments with abundant direct sunlight, as is seen often in diurnal extant birds and mammals [13, 18]. Additionally, it has been suggested that glare is especially high in riparian habitats, because light reflectance is increased by proximity to water, as may have been the case in the lacustrine environment in which *Sinosauropteryx* fossils were deposited [15]. Pigmented bands that run directly across the orbital region may also help to mask the presence of the eyes as a form of camouflage against both predators and potential prey [20, 21]. Eye stripes are common in modern birds, which most often also have dark eyes, making them likely harder for visual predators or prey to detect, and given that eyes elicit responses from both in many situations, it is a plausible hypothesis [13]. Other possible functions of dark patches around the eyes of extant animals include aposematism and intraspecific signaling [13, 17]. Bandit masks have been suggested as



Figure 2. Reconstructed Color Patterns of *Sinosauropteryx*

(A) Schematic based on the distribution of pigmented plumage in NIGP 127586 and NIGP 127587 highlighting the level of the countershading transition from a dark dorsum to light ventrum. Scale bar represents 100 mm.

(B) Reconstruction of *Sinosauropteryx* in the predicted open habitats in which it lived around the Jehol lakes, preying on the lizard *Dalinghosaurus*.

The tail of *Sinosauropteryx* was the longest of any known theropod relative to body length [24]. Due to this length, it is unlikely that the animal could hold it in a perfectly horizontal position consistently, which would be necessary for a countershaded pattern to be effective. This may explain why the tail is banded rather than showing the countershaded pattern seen on the animal's flanks. The great length of the tail in combination with the distinct and presumably conspicuous color bands may be explained as a distraction strategy, a method of attracting attention as far from the less-conspicuous head and body as possible. Alternatively, the banding could have served as a form of disruptive camouflage, as is seen in a number of modern animals, breaking up the outline of the tail to make it less recognizable to potential predators [15–18]. A combined function of camouflage and intraspecific signaling has also been suggested in some extant bird taxa with banded pat-

terns [25]. However, we find no osteological evidence for an ability to lift or pose the tail, which would have limited its utility in display.

being primarily aposematic in mammalian taxa living in exposed open habitats and are especially prevalent in mammalian carnivores, which co-exist with larger carnivores [17, 22, 23], as is likely to have been the situation for *Sinosauropteryx*. A number of modern mammals combine bandit masks with defensive nauseous discharges [22], but it is not possible to ascertain whether this was the case with *Sinosauropteryx*, and aposematism is generally thought to be rare in modern birds [13], making aposematism unlikely in *Sinosauropteryx*. Alternatively, conspicuous face markings could serve as a warning of a physical deterrent, such as a weapon or armor [17, 22, 23]. Although the theropod had an enlarged claw on each hand [24], the animal's small size makes it unlikely that it posed any real threat to its likely much larger theropod predators, making this function of the bandit mask unlikely.

Function of the Banded Tail

Banded tails are poorly understood in modern animals and likely serve several functions, including social signaling, dazzle camouflage, and outline breaking/disruptive camouflage [15–18]. Banded tails have been proposed as a way of confusing predators or drawing attention away from more vital body parts [18].

Countershading in *Sinosauropteryx*

A clear darker dorsum and absence of pigmented plumage ventrally, with the light ventral side extending to the tail until at least the tenth caudal vertebra, conforms to what would be expected for countershaded camouflage adapted to reduce detection from visual predators and from potential prey [1, 3–5]. Visual hunting was likely important for predators of *Sinosauropteryx*. Several tyrannosauroids are contemporaneous with *Sinosauropteryx* [26]. Although these tyrannosauroids were small for the clade [26], they would likely have been more than capable of tackling the diminutive compsognathid, which appears to have not reached sizes much greater than a meter in length [24]. Modern avian predators rely heavily on their exceptional vision to hunt, and as such it is likely that their forebears, the theropods, also had excellent visual capabilities [27]. It has been shown that a number of tyrannosauroids had visual capabilities similar to modern raptorial birds [28], and as such strong selection for camouflage would have been likely in their prey. In fact,

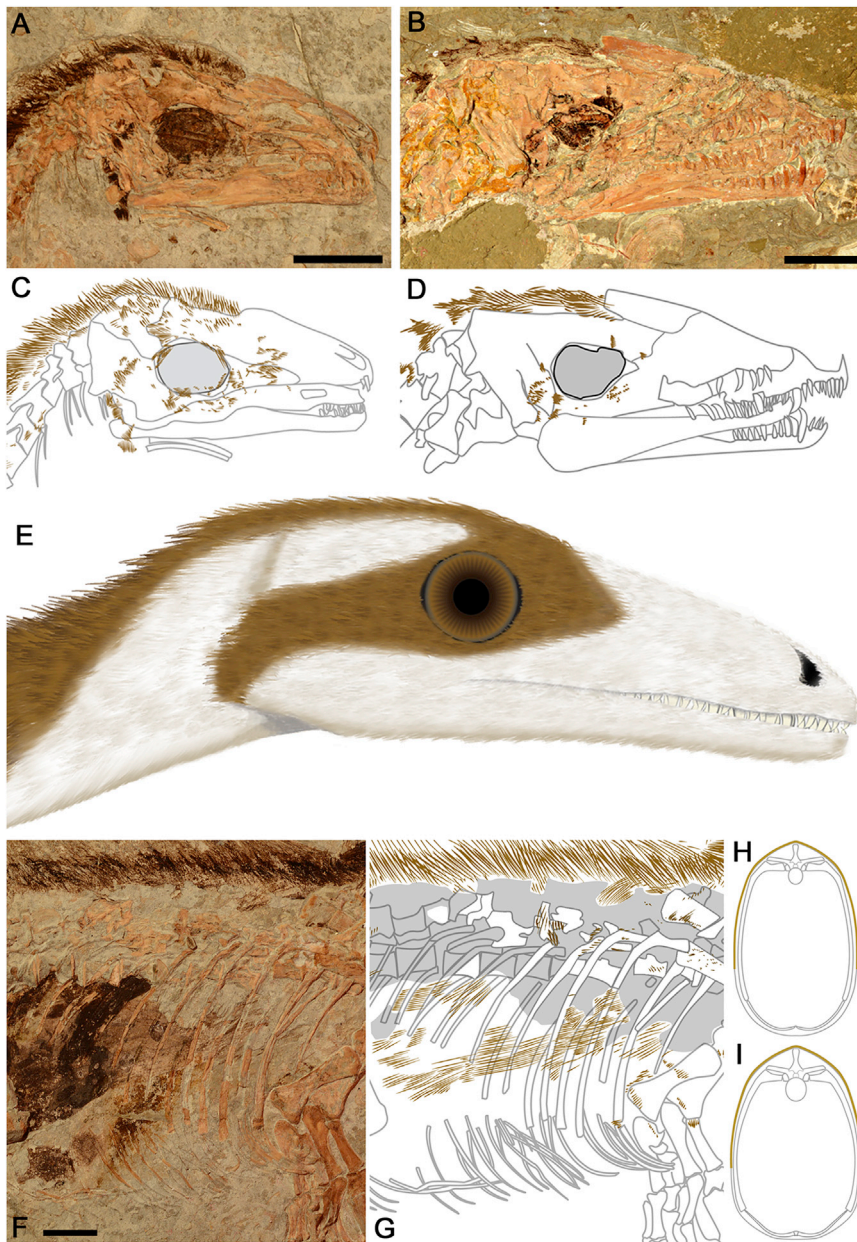


Figure 3. Detail of the Pigmented Plumage Distribution across the Face and Abdomen of *Sinosauropteryx*

(A) The skull of NIGP 127586, showing pigmented feathers forming a crest on the top of the head running along the dorsal side of the neck and patches of plumage on the posteroventral margin of the lower jaw and around the eye orbit. The orbit shows abundant pigment, likely from retinal melanin. Pigmented feathers can also be seen anterior to the orbit and in patches joining those around the orbit to the dorsal crest, indicating a stripe of pigment running across the eye.

(B) The skull of NIGP 127587, showing a similar pigmented plumage distribution to NIGP127586 but with poorer preservation.

(C) Interpretive drawing of the skull of (A) showing the distribution of pigmented feathers.

(D) Interpretive drawing of (B).

(E) Full reconstruction of the head of *Sinosauropteryx* based on the distribution of the plumage in the two specimens. This pattern conforms to a “bandit mask,” seen in many modern taxa.

(F) The abdomen of NIGP 127586, showing feather filaments running across internal melanized soft tissues.

(G) Interpretive drawing of the abdomen of NIGP 127586, showing the ventral extent of feathers (brown) and overlying sediment covering feathers dorsally (gray area).

(H) Transverse section of NIGP 127586, showing the proposed ventral extent of pigmented plumage (brown).

(I) Transverse section of NIGP 127587, showing the proposed ventral pigmented plumage extent. Scale bars represent 20 mm in (A)–(D) and 10 mm in (F) and (G). Reconstruction and transverse sections are not to scale.

considering that theropods were most likely tri- or tetra-chromatic, like their extant counterparts the tetrachromatic birds [29, 30] and the trichromatic crocodiles [31], the Mesozoic predator-prey dynamic would likely have been much more visual than extant terrestrial biotas in which dichromatic mammals are highest in the food chain. It is therefore not surprising to observe camouflage patterns in a small Cretaceous theropod.

Although many of the vertebrates of the Jehol Biota were arboreal or scansorial, including a number of other theropods [11], owing to its anatomy *Sinosauropteryx* was likely restricted to an obligate terrestrial habit and thus did not have the option of retreating to the trees to escape predators. Further, color patterns beneficial as camouflage would have aided *Sinosauropteryx* in hunting its own prey, which likely also relied, at least in

part, on visual cues to detect predators. The hypothesis that its color patterning was predominantly driven by a need to remain cryptic is therefore parsimonious in *Sinosauropteryx*. Alternative explanations for countershading in modern animals, such as thermoregulation, UV protection, and the costs of producing pigmentation, could also play a role in the color patterns observed in *Sinosauropteryx*. The relative importance of these possible functions and their interplay in modern animals is, however, poorly understood, and thus would be difficult to explore in an extinct animal. Despite potential limitations in our understanding of countershading function in modern animals, the correlation between habitat and countershading pattern nuances has been quantitatively shown in numerous extant taxa and was likely also present in the past.

Habitat Preference

The Jehol Biota includes abundant and diverse floral remains alongside its fauna [11, 32]. High paleotemperatures may have aided the development of lush forested habitats thought to have existed in much of the area [11]. Speculation has been

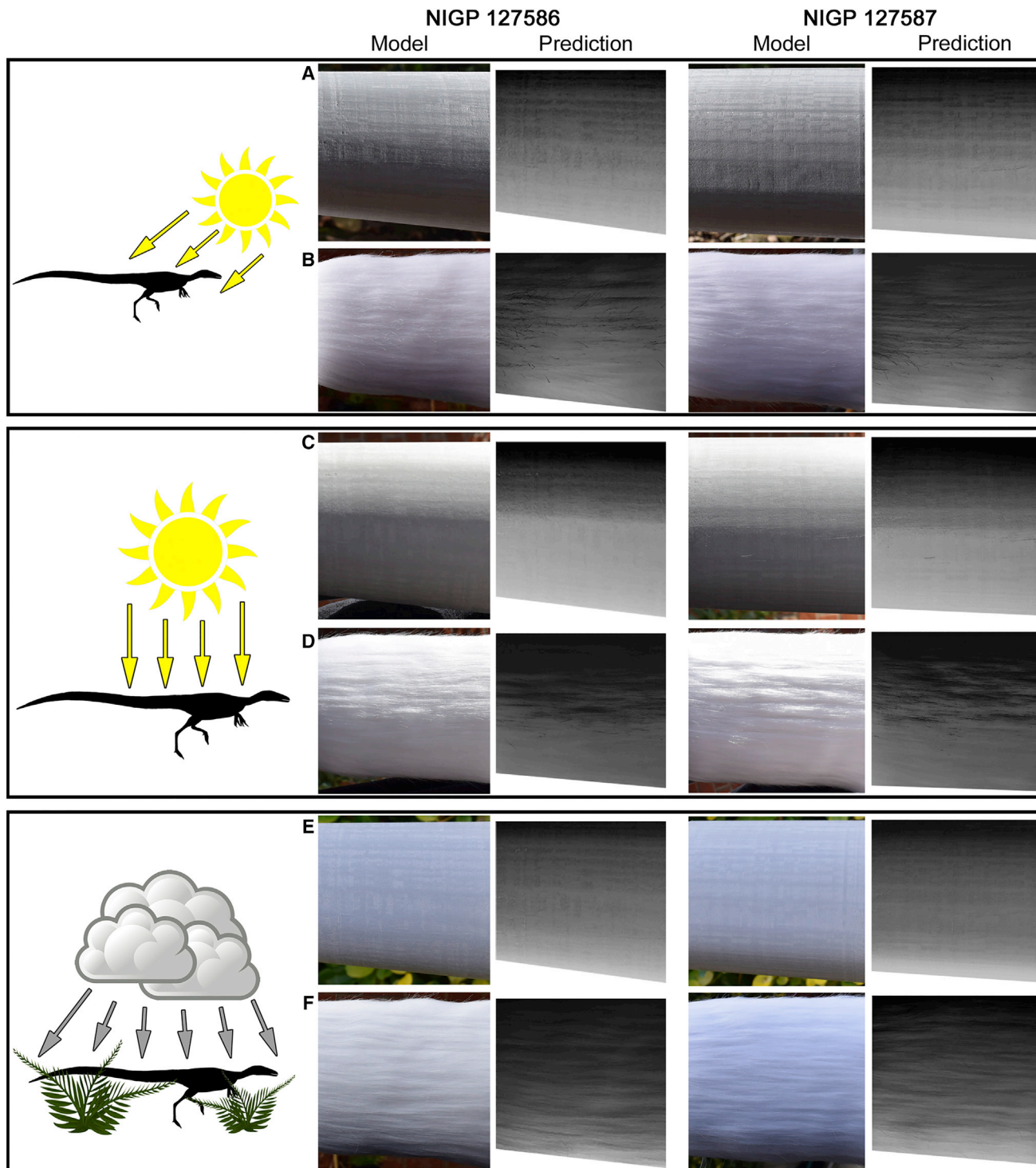


Figure 4. The Differing Pattern of Predicted Self-Shadowing in *Sinosauropteryx*

3D models of the abdomen of NIGP 127586 and NIGP 127587 imaged under different lighting conditions. “Model” represents the original photographs taken of the models to show how the self-shadows are cast across each, with and without synthetic fur added as a feather analog. “Prediction” shows how a gradient of pigment dorsoventrally would be expected to perfectly counterbalance the illumination gradient caused by self-shadowing.

(A and B) Direct sunlight at an altitude of around 30° on smooth and “feathered” models.

(C and D) Direct sunlight at an altitude of 90° on smooth and “feathered” models.

(E and F) Diffuse lighting under 100% cloud cover (which equates to a closed environment) on smooth and “feathered” models.

The ventral position and sharpness of the predicted countershading transition can be seen to be higher and sharper under overhead direct lighting, indicative of an open environment (C and D), whereas under diffuse lighting, representing a closed habitat, the transition is lower and more gradual (E and F).

made about certain taxa inhabiting more- or less-densely forested areas [11], and owing to the volcanic nature of the deposits it is likely that a mosaic of habitats existed in the region, with open areas occurring among denser forested regions [32]. The paleobotanical record of Jehol shows plants adapted for both arid and humid environments, suggesting climatic fluctuations through time [12]. Because all paleobotanical remains are allochthonous with no *in situ* plant fossils known, it is likely that different plant communities existed in the regions around the Jehol lakes and further afield [12].

It has been proposed that the larger theropods of Jehol would likely have been found in more open areas, where vegetation was less likely to impede their movement [11]. The countershading pattern of *Sinosauropteryx* indicates that it, too, inhabited these more open areas where predation pressure may have been significantly higher due to reduced cover than in the closed areas and where background-matching camouflage was more difficult to achieve. A need to reduce conspicuousness relative to the environment would therefore have been important to avoid detection from keen visual predators. The diminutive size of *Sinosauropteryx* and its relatively high countershading transition adapted for open areas indicates that it lived in habitats with either few plants or very low vegetation cover.

Further insight may come from the lizard in the stomach of NIGP 127587 (Figures 1D and 1E and S2). Of the known Jehol lizard fauna, the preserved skeletal elements most closely match those of *Dalinghosaurus*, found in the same deposits as *Sinosauropteryx* (the Yixian Formation) [33, 34]. The tail and hind limbs of *Dalinghosaurus* are exceptionally long relative to its forelimbs, which in modern lizards is a typical morphology of fast-moving terrestrial runners, potentially capable of bipedal locomotion at high speed [34, 35]. Shorter limbs are generally associated with arboreality [35]. Although the slender ungual phalanges of *Dalinghosaurus* indicate that it was likely capable of climbing [33], it appears likely it was better suited to living in the same open habitats inferred herein for the theropod.

Most groups of terrestrial vertebrates in Jehol show a strong tendency toward forest-living adaptations [11]. *Sinosauropteryx*, however, appears to be an exception to this rule. The insight that small theropods like *Sinosauropteryx* may have inhabited open habitats helps build a clearer picture of the environment in which the Jehol animals lived. Jehol clearly was not only rich taxonomically, but was also likely varied in the habitats available to animals and consisted of a mosaic of environments, which may explain the area's extraordinary biodiversity [32]. Furthermore, the Jehol biota straddles more than 10 million years and is likely to have fluctuated in vegetation cover and landscape. Arboreal taxa and dinosaurs adapted in their color patterning to closed habitats were present in the forested areas [3, 9, 11] while larger dinosaurs and their smaller cryptically patterned prey explored open areas with less-dense vegetation. The presence of dinosaurs showing camouflage patterns adapted to different habitats indicates that the environment around the Jehol lakes was therefore diverse and varied and hosted different dinosaurian faunas. We have shown how a greater understanding of ancient environments can come from better understanding of the paleoecology of extinct animals through paleocolor reconstructions. This work furthers our

understanding of how color patterns have evolved through time and highlights the importance of anti-predator camouflage strategies in deep time.

STAR★METHODS

Detailed methods are provided in the online version of this paper and include the following:

- KEY RESOURCES TABLE
- CONTACT FOR REAGENT AND RESOURCE SHARING
- METHOD DETAILS
 - Institutional Abbreviations
 - Specimen Imaging
 - 2D Illustrations and Plumage Distribution
 - 3D Abdominal Modeling
 - Predicting Lighting Environment
- QUANTIFICATION AND STATISTICAL ANALYSIS
 - Quantification of Countershading Transition
- DATA AND SOFTWARE AVAILABILITY

SUPPLEMENTAL INFORMATION

Supplemental Information includes two figures and Supplemental Descriptions and can be found with this article online at <https://doi.org/10.1016/j.cub.2017.09.032>.

A video abstract is available at <https://doi.org/10.1016/j.cub.2017.09.032#mmc3>.

AUTHOR CONTRIBUTIONS

F.M.S. produced all illustrations and the reconstruction in Figure 2A, created and imaged the 3D models, and wrote the manuscript. J.V. devised the project concepts and imaged the fossils. R.N. produced the full art reconstruction in Figure 2B. I.C.C. produced the MATLAB models and performed the statistical analyses of countershading predictions versus the reconstruction. All authors commented on the manuscript.

ACKNOWLEDGMENTS

We would like to thank Yunbai Zhang and Diying Huang for access and help with specimens. We also thank Nick Longrich for discussion. F.M.S. was funded by the Natural Environment Research Council (PhD grant NE/L002434/1).

Received: May 18, 2017

Revised: August 14, 2017

Accepted: September 14, 2017

Published: October 26, 2017

REFERENCES

1. Allen, W.L., Baddeley, R., Cuthill, I.C., and Scott-Samuel, N.E. (2012). A quantitative test of the predicted relationship between countershading and lighting environment. *Am. Nat.* 180, 762–776.
2. Thayer, A.H. (1896). The law which underlies protective coloration. *Auk* 13, 124–129.
3. Vinther, J., Nicholls, R., Lautenschlager, S., Pittman, M., Kaye, T.G., Rayfield, E., Mayr, G., and Cuthill, I.C. (2016). 3D camouflage in an ornithischian dinosaur. *Curr. Biol.* 26, 2456–2462.
4. Rowland, H.M. (2009). From Abbott Thayer to the present day: what have we learned about the function of countershading? *Philos. Trans. R. Soc. Lond. B Biol. Sci.* 364, 519–527.

5. Cuthill, I.C., Sanghera, N.S., Penacchio, O., Lovell, P.G., Ruxton, G.D., and Harris, J.M. (2016). Optimizing countershading camouflage. *Proc. Natl. Acad. Sci. USA* *113*, 13093–13097.
6. Penacchio, O., Lovell, P.G., Cuthill, I.C., Ruxton, G.D., and Harris, J.M. (2015). Three-dimensional camouflage: exploiting photons to conceal form. *Am. Nat.* *186*, 553–563.
7. Vinther, J. (2015). A guide to the field of palaeo colour: Melanin and other pigments can fossilise: Reconstructing colour patterns from ancient organisms can give new insights to ecology and behaviour. *BioEssays* *37*, 643–656.
8. Vinther, J., Briggs, D.E., Prum, R.O., and Saranathan, V. (2008). The colour of fossil feathers. *Biol. Lett.* *4*, 522–525.
9. Li, Q., Gao, K.-Q., Meng, Q., Clarke, J.A., Shawkey, M.D., D’Alba, L., Pei, R., Ellison, M., Norell, M.A., and Vinther, J. (2012). Reconstruction of *Microraptor* and the evolution of iridescent plumage. *Science* *335*, 1215–1219.
10. Li, Q., Gao, K.-Q., Vinther, J., Shawkey, M.D., Clarke, J.A., D’Alba, L., Meng, Q., Briggs, D.E., and Prum, R.O. (2010). Plumage color patterns of an extinct dinosaur. *Science* *327*, 1369–1372.
11. Zhonghe, Z. (2006). Evolutionary radiation of the Jehol Biota: chronological and ecological perspectives. *Geol. J.* *41*, 377–393.
12. Barrett, P.M., and Hilton, J.M. (2006). The Jehol Biota (Lower Cretaceous, China): new discoveries and future prospects. *Integr. Zool.* *1*, 15–17.
13. Bortolotti, G.R., Hill, G., and McGraw, K. (2006). Natural selection and coloration: protection, concealment, advertisement, or deception. In *Bird Coloration, Volume 2*, pp. 3–35.
14. Ficken, R.W., and Wilmot, L.B. (1968). Do facial eye-stripes function in avian vision? *Am. Midl. Nat.* *79*, 522–523.
15. Ortolani, A. (1999). Spots, stripes, tail tips and dark eyes: predicting the function of carnivore colour patterns using the comparative method. *Biol. J. Linn. Soc. Lond.* *67*, 433–476.
16. Caro, T. (2005). The adaptive significance of coloration in mammals. *Bioscience* *55*, 125–136.
17. Caro, T. (2009). Contrasting coloration in terrestrial mammals. *Philos. Trans. R. Soc. Lond. B Biol. Sci.* *364*, 537–548.
18. Caro, T. (2013). The colours of extant mammals. *Semin. Cell Dev. Biol.* *24*, 542–552.
19. Smithwick, F.M., Mayr, G., Saitta, E.T., Benton, M.J., and Vinther, J. (2017). On the purported presence of fossilized collagen fibres in an ichthyosaur and a theropod dinosaur. *Palaeontology* *60*, 409–422.
20. Cuthill, I.C., and Székely, A. (2009). Coincident disruptive coloration. *Philos. Trans. R. Soc. Lond. B Biol. Sci.* *364*, 489–496.
21. Kjærsmo, K., Grönholm, M., and Merilaita, S. (2016). Adaptive constellations of protective marks: eyespots, eye stripes and diversion of attacks by fish. *Anim. Behav.* *111*, 189–195.
22. Newman, C., Buesching, C.D., and Wolff, J.O. (2005). The function of facial masks in “midguild” carnivores. *Oikos* *108*, 623–633.
23. Stankowich, T., Caro, T., and Cox, M. (2011). Bold coloration and the evolution of aposematism in terrestrial carnivores. *Evolution* *65*, 3090–3099.
24. Currie, P.J., and Chen, P.-j. (2001). Anatomy of *Sinosauropteryx prima* from Liaoning, northeastern China. *Can. J. Earth Sci.* *38*, 1705–1727.
25. Marques, C.I., Batalha, H.R., and Cardoso, G.C. (2016). Signalling with a cryptic trait: the regularity of barred plumage in common waxbills. *R. Soc. Open Sci.* *3*, 160195.
26. Zhou, Z., and Wang, Y. (2010). Vertebrate diversity of the Jehol Biota as compared with other lagerstätten. *Sci. China Earth Sci.* *53*, 1894–1907.
27. Hart, N.S. (2001). The visual ecology of avian photoreceptors. *Prog. Retin. Eye Res.* *20*, 675–703.
28. Stevens, K.A. (2006). Binocular vision in theropod dinosaurs. *J. Vertebr. Paleontol.* *26*, 321–330.
29. Bowmaker, J.K. (1980). Colour vision in birds and the role of oil droplets. *Trends Neurosci.* *3*, 196–199.
30. Vorobyev, M., Osorio, D., Bennett, A.T., Marshall, N.J., and Cuthill, I.C. (1998). Tetrachromacy, oil droplets and bird plumage colours. *J. Comp. Physiol. A Neuroethol. Sens. Neural Behav. Physiol.* *183*, 621–633.
31. Nagloo, N., Collin, S.P., Hemmi, J.M., and Hart, N.S. (2016). Spatial resolving power and spectral sensitivity of the saltwater crocodile, *Crocodylus porosus*, and the freshwater crocodile, *Crocodylus johnstoni*. *J. Exp. Biol.* *219*, 1394–1404.
32. Zhou, Z., Barrett, P.M., and Hilton, J. (2003). An exceptionally preserved Lower Cretaceous ecosystem. *Nature* *421*, 807–814.
33. Evans, S.E., and Wang, Y. (2005). The early cretaceous lizard *Dalinghosaurus* from China. *Acta Palaeontol. Pol.* *50*, 725–742.
34. Shu’an, J., and Qiang, J. (2004). Postcranial anatomy of the Mesozoic *Dalinghosaurus* (Squamata): evidence from a new specimen of western Liaoning. *Acta Geol. Sin.-Engl.* *78*, 897–905.
35. Olberding, J.P., Herrel, A., Higham, T.E., and Garland, T. (2015). Limb segment contributions to the evolution of hind limb length in phrynosomid lizards. *Biol. J. Linn. Soc. Lond.* *117*, 775–795.
36. Blender, version 2.78. (Blender Foundation). <https://www.blender.org>.
37. MATLAB and Statistics Toolbox, release R2016a. (MathWorks). <https://www.mathworks.com/products/matlab.html>.
38. R Core Team (2015). R: A language and environment for statistical computing (R Foundation for Statistical Computing). <https://www.r-project.org/>.
39. Bates, D., Mächler, M., Bolker, B., and Walker, S. (2015). Fitting Linear Mixed-Effects Models using lme4. *J. Stat. Softw.* *67*, 1–48.
40. Bengtson, S. (2000). Teasing fossils out of shales with cameras and computers. *Palaeontol. Electronica* *3*, 14.
41. Boyle, B. (1992). Fossil detail leaps with double polarization. *Professional Photographers of Canada* *22*, 10–12.
42. Rayner, R.J. (1992). A method of improving contrast in illustrations of coalified fossils. *Palaeontol. Afr.* *29*, 45–49.
43. Colleary, C., Dolocan, A., Gardner, J., Singh, S., Wuttke, M., Rabenstein, R., Habersetzer, J., Schaal, S., Feseha, M., Clemens, M., et al. (2015). Chemical, experimental, and morphological evidence for diagenetically altered melanin in exceptionally preserved fossils. *Proc. Natl. Acad. Sci. USA* *112*, 12592–12597.
44. Zhang, F., Kearns, S.L., Orr, P.J., Benton, M.J., Zhou, Z., Johnson, D., Xu, X., and Wang, X. (2010). Fossilized melanosomes and the colour of Cretaceous dinosaurs and birds. *Nature* *463*, 1075–1078.
45. Prum, R.O., and Williamson, S. (2002). Reaction-diffusion models of within-feather pigmentation patterning. *Proc. Biol. Sci.* *269*, 781–792.

STAR★METHODS

KEY RESOURCES TABLE

REAGENT or RESOURCE	SOURCE	IDENTIFIER
Software and Algorithms		
Blender version 2.78	[36]	https://www.blender.org
MATLAB version R2016a	[37]	https://www.mathworks.com/products/matlab.html
R version 3.4.0	[38]	http://www.r-project.org/
R package lme4	[39]	https://cran.r-project.org/web/packages/lme4/index.html

CONTACT FOR REAGENT AND RESOURCE SHARING

Further information and requests for resources and reagents should be directed to and will be fulfilled by the Lead Contact, Jakob Vinther (jakob.vinther@bristol.ac.uk).

METHOD DETAILS

Institutional Abbreviations

GMV – Vertebrate Collections of the Geological Museum of China, Beijing; NIGP – Nanjing Institute of Geology and Palaeontology, Chinese Academy of Sciences, Nanjing, Jiangsu Province; IVPP – Institute of Vertebrate Palaeontology and Palaeoanthropology, Chinese Academy of Sciences, Beijing.

Specimen Imaging

Three of the best preserved specimens of *Sinosauropteryx* (NIGP 127586, NIGP 127587, and IVPP V12415; [Figures 1A and 1D and S1A](#)) were imaged using a Nikon D800 camera with a Micro Nikkor 60 mm macro lens and polarizing filter attached. The camera was mounted on a tripod and a ten second delayed timer used to maximize image sharpness. TIFF format (5520 × 3680 pixels) was used to capture the images in high resolution. Specimens were illuminated with a mounted tungsten light source (Lowell Tota-light, Tiffen, Hauppauge, NY, USA) with a linear polarizing gel attached. Images were taken under both normal lighting conditions and using the polarized filter on the camera adjusted to allow cross-polarization to reduce glare from the specimen [40–42].

2D Illustrations and Plumage Distribution

Illustrations of specimens NIGP 127586 and NIGP 127587 were created using Adobe Illustrator (Adobe, San Jose, CA, USA), as these specimens show the best preservation of the integument and are the most articulated. Separate layers were drawn for the skeleton, internal soft tissue and feathers. Feathers were mapped across each specimen, with particular attention paid around the abdomen to ensure that the ventral extent of the preserved plumage was accurately depicted. Across the stomach region, other soft tissues are preserved which likely represent remains of internal organs, which are known to contain the pigment melanin [7]. Differentiating between organ melanin and feather melanin is possible as the feathers can be seen preserved on top of the internal soft tissues as clear linear features representing filaments ([Figures 3F and 3G](#)).

Two forms of melanin are found in modern feathers both of which are known to survive in fossils; eumelanin which is packaged inside eumelanosomes and phaeomelanin found in phaeomelanosomes [43]. Previous work identified preserved pigment remains in the feathers of another reported *Sinosauropteryx* specimen IVPP 14202 in the form of phaeomelanosomes, indicating that the pigmented plumage was likely a rufous or light brown tone [44]. Caution must be taken, however, in reconstructing color patterns across an animal from single, small spot samples between individual fossil specimens. Unfortunately, IVPP 14202 was not available for this study. Here, we focus on the distribution of pigmentation in the plumage and its overall pattern across the body rather than further attempting to accurately reconstruct the original hues of the animal. As the pigment appears to be restricted to the feathers in *Sinosauropteryx*, the complexities of color production found in other integumentary structures, such as the chromatophores found in the skin of reptiles [7], do not apply in this case. Melanosomes are transported to the feather keratin as it develops after which time it cannot be altered (other than through bleaching) [45]. Pigment remains in the fossil should therefore represent the original distribution of melanin in the animal's plumage at the time of death.

3D Abdominal Modeling

From the illustrations of NIGP 127586 and NIGP 127587, the best preserved ribs, gastralia and vertebrae from the anterior end of each animal's abdomen were used to create two-dimensional reconstructions of the ribcages in cross section ([Figures 1C and 1F](#)). The ribs and gastralia were mirrored for symmetry from single bones in each specimen. A layer representing the skin and musculature of the

abdomen was added around the bones. The extent of the tissues surrounding the abdominal skeleton is unknown, but from the proximity of the feathers to the bones across the fossils and through comparison to modern animals we consider it likely that musculature was minimal in this region and therefore the cross section of the abdomen would match well to the shape of the bones themselves, minimizing any effects of overlying tissue being over or underestimated. The outlines of the abdominal cross sections were used to create 3D reconstructions of the abdomen of each individual using the software Blender [36]. The abdomen length and height (both posterior and anterior) were taken directly from the fossils and the width was extrapolated from the curvature of the ribs and gastralia. This method produced consistent relative proportions in each model despite a difference in the overall size of each. Each abdomen was taller at the posterior end than the anterior in both specimens, and so the models were tapered according to the exact dimensions measured from each fossil (6% in NIGP 127587 and 15% in NIGP 127586). The difference in the degree of tapering may represent ontogenetic differences, as NIGP 127586 is a much smaller individual than NIGP 127587. The two 3D models were then printed by Shapeways (New York, NY, USA) in gray polylactic acid (PLA) and sanded using increasing grit sandpaper to smooth the surfaces. To replicate the feathers, unicolor synthetic fur (White Ape, Mohair Bear Making Supplies Ltd, Telford, Shropshire, UK) was used to wrap around each model and the filament length trimmed based on the lengths of the feather filaments measured from each fossil.

Predicting Lighting Environment

The 3D models of the two *Sinosauropteryx* abdomens were printed uniformly gray to allow assessment of the position of self-shadows depending on different lighting conditions, independent of actual color patterns [1, 3]. The models were mounted on sticks attached horizontally to a tripod to avoid any shadows being cast across them from other objects. The two models were photographed under different lighting conditions, similar to the recent study of *Psittacosaurus* [3]. A Nikon D5300 SLR camera with an 18-55 mm Nikkor lens (Nikon Corporation, Tokyo, Japan) was used for imaging with the light metering set on the center of the model and automatic focus used. Images were saved in TIFF format. A color standard (X-Rite Color Passport; X-Rite Inc. Grand Rapids, MI, USA) was positioned next to and in the same plane as the model. Photographs were taken at the University of Bristol Botanical Gardens at around midday (\pm two hours) on sunny ($< 10\%$ cloud cover) and cloudy (complete cloud cover) days in both open and closed environments. The area chosen was populated by plants typical of the Early Cretaceous. The models were placed facing directly toward the sun in both instances, as this is the situation in which symmetrical countershading will be most effective as the illumination gradient will be the same on both flanks [1]. Previous work has shown that due to variability in the sun's position and the effect that will have on illumination gradients, modern ungulates often show countershading patterns which are a compromise between the range of lighting conditions in which each taxon lives where predation pressure will be experienced [1]. Each model was therefore also imaged at an angle perpendicular to the sun, with the dorsal side receiving direct illumination to imitate the sun being directly overhead. The models were imaged both as gray uncoated plastic and with the synthetic fur tightly wrapped around to test for any differences in the illumination gradients with and without feathers (Figure 4). As with previous work, the shadows cast reduced to two illumination conditions (direct and diffuse) corresponding to whether the light was coming directly from the sun's disk or the sky. Consequently, images taken under cloudy conditions produced the same shadowing patterns as those taken in sunlight under vegetation, making them equivalent, for predictions, to a closed habitat. After imaging, the models were cropped and the lighting inverted to show where the optimal countershading transition should fall for each lighting condition in order to counterbalance the illumination gradient and thus minimize conspicuousness through self-shadow obliteration (Figure 4). This was carried out in MATLAB (2016a) [37]. The predicted countershading transitions were then directly compared to the reconstructed color patterns across the abdomens of both *Sinosauropteryx* specimens (Figures 2 and 3H and 3I).

QUANTIFICATION AND STATISTICAL ANALYSIS

Quantification of Countershading Transition

Confidence intervals for the transition points to a lighter belly were estimated as follows. First, transects of the calibrated intensity were taken from dorsal to ventral side. For each transect a cubic spline with 7 degrees of freedom was fitted as a smoother using function `smooth.spline()` in R 3.4.0 [38]. Smoothing was necessary, particularly for the fur-covered models which showed spatial heterogeneity due to irregularities in the lie of the fur; 7 d.f. adequately captured the general trend in gradient without too much smoothing. The point along each transect, in pixels, at which the gradient flattened out was located and converted to a percentage of the distance from dorsal to ventral side. Such estimates were calculated for five replicates of each illumination condition (90° direct sun, 30° direct sun and diffuse illumination), integument (“skin” or “feathers”) and model ($n = 2$). The mean and 95% profile confidence intervals for each illumination condition were estimated using a Linear Mixed Model (Gaussian error) with random effects “model” and “integument”. The model was fitted using function `lmer` in package `lme4` [39] in R. The final calculated confidence intervals can be found in the Results.

DATA AND SOFTWARE AVAILABILITY

Data supporting this study are provided within the paper and supplemental material.